



# Theoretical insights on C-N coupling mechanism and guidance for screening the catalysts of electrocatalytic urea synthesis by descriptors

Meng Zheng<sup>a,b</sup>, Haiqing Ma<sup>a</sup>, Zhiming Li<sup>a</sup>, Hongan Yu<sup>a</sup>, Long Nie<sup>a</sup>, Chenliang Ye<sup>a,b</sup>, Xiaoyu Chen<sup>a,b</sup>, Jin Wang<sup>a,\*</sup>

<sup>a</sup> College of Materials Science and Engineering, Shenzhen University, Shenzhen 518071, China

<sup>b</sup> College of Physics and Optoelectronic Engineering, Shenzhen University, Shenzhen 518060, China

## ARTICLE INFO

**Keywords:**  
Electrocatalytic  
Urea synthesis  
Descriptors  
C-N coupling  
Density functional theory

## ABSTRACT

Electrocatalytic urea synthesis from CO<sub>2</sub> and nitrate/nitrite is promising as a sustainable strategy to alleviate the dependency on fossil resources and CO<sub>2</sub> release. The complicated synthesis steps and controversial C-N coupling mechanism restrict the design of efficient catalysts to satisfy industrial application. Herein, based on density functional theory calculations on metals (Au, Ag, Pd, Cu, and Ni) and micro-kinetic analysis, the C-N coupling mechanism is clarified as CO<sub>2</sub>+ N<sub>1</sub> species (NO\*, NOH\*, or N\*). The formed chemical adsorption of CO<sub>2</sub> on the surface is found as an indicator to directly exclude the inactive metal catalysts. Furthermore, the descriptors of hydrogen and oxygen adsorption energy are successfully related to the catalysis performance, and the catalysts with moderate hydrogen adsorption and strong oxygen adsorption strength are predicted with the outstanding performance, which is validated by the experimental results. These insights would be helpful to identify and design high-performance catalysts for electrocatalytic urea synthesis.

## 1. Introduction

Urea is an important artificial nitrogen fertilizer and the crops using urea feed around 20% of the world population [1]. Currently, the required ammonia for the production of urea heavily relies on Haber-Bosch technology, in which 1–2% of the global energy is consumed and around 1% of total energy-related CO<sub>2</sub> in the world is released [2,3]. Electricity-powered synthesis of urea from discarded CO<sub>2</sub> and nitrate/nitrite is a sustainable process, which alleviates the dependency of fossil resources and eliminates the environmental pollution [4–6]. Furthermore, a decentralized and on-site production of urea via electrochemical technology highly improves the application flexibility and reduces the transportation cost.

In 1990 s, Shibata et. al. comprehensively investigated the electrochemical synthesis of urea by co-reduction of CO<sub>2</sub> and nitrate/nitrite on a series of metals and metallophthalocyanine at gas-diffusion electrodes [7–11]. The results show that the Faradaic efficiency of urea formation by nitrite is higher than nitrate, and the maximum Faradaic efficiency could reach up to 55% on both cadmium and zinc electrodes by co-reducing CO<sub>2</sub> and nitrite [8,9]. With the increased demand for sustainable development and advances in electrocatalysis, this type of

reaction has recaptured the attention of researchers in recent years. Various types of catalysts including metals, oxides, hydroxide, single atom catalysts were applied to electrochemical urea formation [12–32]. Despite of tremendous efforts to engineer the electrocatalysts, the present urea Faradaic efficiency is far from that required in industrial application. The mechanism of C-N bond formation is still controversial [33,34], which limits the design of efficient catalysts. Experimentally, the C-N bond formation mechanism has been demonstrated as coupled between CO\* and NH<sub>2</sub>\*(Te-Pd NCs [22], Cu@Zn [29], Co-NiO<sub>x</sub>@GDY [23], TiO<sub>2</sub>-Nafion-modified ITO [19], Cu-N<sub>4</sub> [17], carbon nanotubes with fluorine-rich surface [30]), CO\* and NH\*(Fe-Ni-N<sub>6</sub> [26]), COOH\* and NH<sub>2</sub>\*(ZnO-Vo [18]), CO\* and NH<sub>2</sub>OH\*(AuPd [31]), CO<sub>2</sub>\* and NO<sub>2</sub>\* (In(OH)<sub>3</sub> [20], V<sub>o</sub>-InOOH [32]), and so on. Theoretically, for Cu catalysts, Qiao et. al. suggested that CO\* and NH\* form C-N bond at low potential and the C-N bonding occurs between solvated CO and NH\* at high potential [35]. However, Cheng et. al. proposed that C-N coupling is derived from CO<sub>2</sub> and N<sub>1</sub>\* species [36]. Overall, it is significant to determine the C-N coupling mechanism of electrochemical synthesis of urea based on a comprehensive investigation.

Besides, appropriate descriptors are helpful for high-throughput screening of efficient catalysts. The adsorption energies of hydrogen

\* Corresponding author.

E-mail address: [wangjin19@szu.edu.cn](mailto:wangjin19@szu.edu.cn) (J. Wang).

and oxygen atoms have been widely used as the descriptors of hydrogen evolution reaction (HER) and oxygen evolution reaction (OER) respectively, to relate to the catalysis performance [37,38]. Great efforts have also been made to find the descriptors of individual  $\text{CO}_x$  and  $\text{NO}_x$  reduction [39,40]. However, there is lack of research about descriptors of electrochemical formation of urea by  $\text{CO}_2$  and nitrate/nitrite. This reaction is very complicated including multiple electrochemical and non-electrochemical steps. Hence, this work is also dedicated to identify the descriptors of urea formation by  $\text{CO}_2$  and nitrate/nitrite.

Therefore, this work is aimed to study the electrochemical (reduction of  $\text{CO}_2$  and nitrate/nitrite) and non-electrochemical (first C-N coupling) steps on metal surfaces (Au, Ag, Pd, Cu, and Ni) based on density functional theory (DFT). Cu and Ag display more effective catalysis performance for urea synthesis than Au, Pd, and Ni [9]. Previous research suggest that Cu(100) is the major active facet under the reduction reaction conditions similar to electrocatalytic urea synthesis [35,41–44] and Ag(100) is possible to be the important facet to complete urea formation due to the impressive performance for  $\text{CO}_2$  to CO [8,45]. Hence, this work selected M(100) surface as model to study C-N formation mechanism. It is found that the adsorption energies of hydrogen and oxygen atoms can serve as the descriptor to relate the involved adsorption energies, reaction energies, and energy barriers. The micro-kinetic analysis reveals the most possible C-N bonding mechanism. Finally, according to the descriptors and reaction mechanism, the suggestions of screening of catalysts are concluded and verified by the reported experimental results.

## 2. Computational details

In this work, the investigated metals (Au, Ag, Pd, Cu, and Ni) are face-centered cubic (fcc) crystals. The (100) surface is selected to model active sites (Fig. S1 shows the cell and model structures of Cu as an example). The models were constructed with four  $3 \times 3$  layers thick metal slab. To save computational source, the top two layers and surface-bound species were allowed to relax, while the bottom two layers were fixed in its bulk position for all the calculations. The periodic models in the z-direction were separated by 15 Å vacuum layer to avoid the interactions between them. To compute the energy of involved molecules, a  $20 \times 20 \times 20 \text{ \AA}^3$  cubic simulation box is employed.

All periodic DFT calculations were performed with the Vienna Ab initio Simulation Package (VASP) on the basis of projector augmented wave (PAW) potentials and the Perdew-Burke-Ernzerhof (PBE) functional [46,47]. The cutoff energy of the plane wave basis was set as 450 eV. For structural optimization, the convergence criteria were  $1 \times 10^{-5}$  eV for energy and  $1 \times 10^{-2}$  eV/Å for force. The spin polarization and dipole corrections were considered during calculation. DFT-D3 method was adopted to correct the van der Waals (vdW) interactions. The Brillouin zone was sampled by the  $3 \times 3 \times 1$  k-point mesh of the Monkhorst-Pack scheme. The transition states were searched by combining climbing-image nudged elastic band (CI-NEB) and dimer methods [48,49]. The searched transition states were verified by imaginary frequency analysis. The adsorption energies, reaction energies, and energy barriers were calculated based on the equations as follows:

$$\Delta E = E_{(\text{catalyst+molecule})} - E_{(\text{molecule})} - E_{(\text{catalyst})} \quad (1)$$

$$E_r = E_{\text{FS}} - E_{\text{IS}} \quad (2)$$

$$E_a = E_{\text{TS}} - E_{\text{IS}} \quad (3)$$

$\Delta E$  is the adsorption energy of molecules,  $E_{(\text{catalyst+molecule})}$ ,  $E_{(\text{catalyst})}$ , and  $E_{(\text{molecule})}$  are the energies of molecules adsorbed on the surface of catalyst, the bare surface of catalyst, and the gas-phase molecule, respectively. Specially, the energies of gas-phase molecule for H, O, and N are calculated as half the energies of  $\text{H}_2$ ,  $\text{O}_2$ , and  $\text{N}_2$ , respectively.  $E_r$  and  $E_a$  are the reaction energy and energy barrier of the elementary step.  $E_{\text{IS}}$ ,  $E_{\text{TS}}$ , and  $E_{\text{FS}}$  are the energies of initial states, transition states and

products, respectively. The adsorption energy of  $\text{NO}_x^-$  was calculated by using gaseous  $\text{HNO}_x$  as the reference [50,51]:

$$\Delta E = E_{(\text{NO}_x^-)} - E_{(\text{catalyst})} - E_{(\text{HNO}_x)} + \frac{1}{2}E_{(\text{H}_2)} + \Delta E_{(\text{correct})} \quad (4)$$

Where  $E_{(\text{NO}_x^-)}$  is the total energy of  $\text{NO}_x^-$  adsorbed on the surface of catalysts, and  $E_{(\text{HNO}_x)}$  and  $E_{(\text{H}_2)}$  are the total energy of gaseous  $\text{HNO}_x$  and  $\text{H}_2$ .  $\Delta E_{(\text{correct})}$  is the correction for compensating the energy change of condensation ( $\text{HNO}_{x(\text{g})} \rightarrow \text{HNO}_{x(\text{l})}$ ) and ionization ( $\text{HNO}_{x(\text{l})} \rightarrow \text{H}^+ + \text{NO}_x^-$ ) to indirectly calculate the energy of  $\text{NO}_x^-$ .

The energy potential change of electrochemical steps were corrected according to the computational hydrogen electrode (CHE) model, which was developed by Nørskov et. al. and has been successfully applied in electrocatalysis [38,52]. The energy barrier at an electrode potential U follows the Butler-Volmer formalism [53] (Eq. 5):

$$E_a(U) = E_a(U^0) + \alpha n e(U - U^0) \quad (5)$$

U is the electrode potential on the RHE scale.  $U^0$  is the equilibrium potential at the analogous nonelectrochemical state, and  $E_a(U^0)$  equals  $E_a$  at equilibrium  $\text{H}^+ + \text{e}^- + * \rightleftharpoons \text{H}^*$  conditions. Where n is the number of electrons transferred, and  $\alpha$  was set as 0.5 for the electrochemical steps, which has been usually considered to be a reasonable approximation. The micro-kinetic analysis was performed by means of MKMCXX software [54].

## 3. Results and discussions

### 3.1. The descriptors of C-N coupling over transition metals

As previously reported, the adsorption energies of hydrogen ( $\Delta E_H$ ) and oxygen ( $\Delta E_O$ ) atom are usually applied as the descriptor for the related volcano plots for the catalysts of hydrogen evolution reaction (HER) [37] and oxygen reduction reaction (ORR) [38] activity, respectively, since the involved reactants, intermediates, and products during the reaction process are adsorbed on catalyst surface through hydrogen or oxygen atom. Furthermore, in the more complex reactions, such as  $\text{CO}_x$  hydrogenation reduction reaction, relevant research show that the  $\Delta E_H$  and the adsorption energies of intermediates which adsorb to the metal surface via carbon atom could be described linearly by the adsorption energies of carbon monoxide ( $\Delta E_{\text{CO}}$ ) [39]. Similarly, in  $\text{NO}_x$  hydrogenation reduction reaction, the adsorption energies of nitrogen atom ( $\Delta E_N$ ) is reported to be linearly scaled with the  $\Delta E_H$  and the adsorption energies of intermediates which adsorb to the metal surface via nitrogen atom [40]. Meanwhile, there is good linear relationship between the  $\Delta E_O$  and adsorption energies of intermediates which bond with metal atoms through oxygen atom during both  $\text{CO}_x$  and  $\text{NO}_x$  hydrogenation reduction reaction processes [39,40]. Hence, it could be obtained that volcano plots about reaction rate and selectivity for  $\text{CO}_x$  or  $\text{NO}_x$  hydrogenation reduction reaction can be described as a function of the descriptors  $\Delta E_{\text{CO}}$  and  $\Delta E_O$  for  $\text{CO}_x$ ,  $\Delta E_N$  and  $\Delta E_O$  for  $\text{NO}_x$  [39,40]. The urea formation process by co-reduction of  $\text{CO}_2$  and  $\text{NO}_x$  is more complicated than  $\text{CO}_x$  and  $\text{NO}_x$  hydrogenation reduction reaction ( $\text{CO}_x\text{RR}$  and  $\text{NO}_x\text{RR}$ ) due to the involvement of the carbon-nitrogen compound (Fig. 1). Identification of the activity descriptors would be very useful to assist the screening of efficient catalysts. Therefore, inspired by the research mentioned above [37–40], the  $\Delta E_H$  and  $\Delta E_O$  as descriptors are firstly applied to describe the adsorption energies of species involved during urea formation process including the carbon-nitrogen compounds in this work.

Adsorption of reactants is the first step of heterogeneous catalysis which significantly affects the reaction rate. In this work, the adsorption of reactants  $\text{CO}_2$  and  $\text{NO}_x$  ( $\text{NO}_3^-$  and  $\text{NO}_2^-$ ) on the metal surfaces is investigated. As shown by the adsorption structures (Fig. 2a and Fig. S2),  $\text{CO}_2$  is physically adsorbed on the studied metal surfaces except for Ni, thereby the adsorption energies of chemically adsorbed hydrogen or

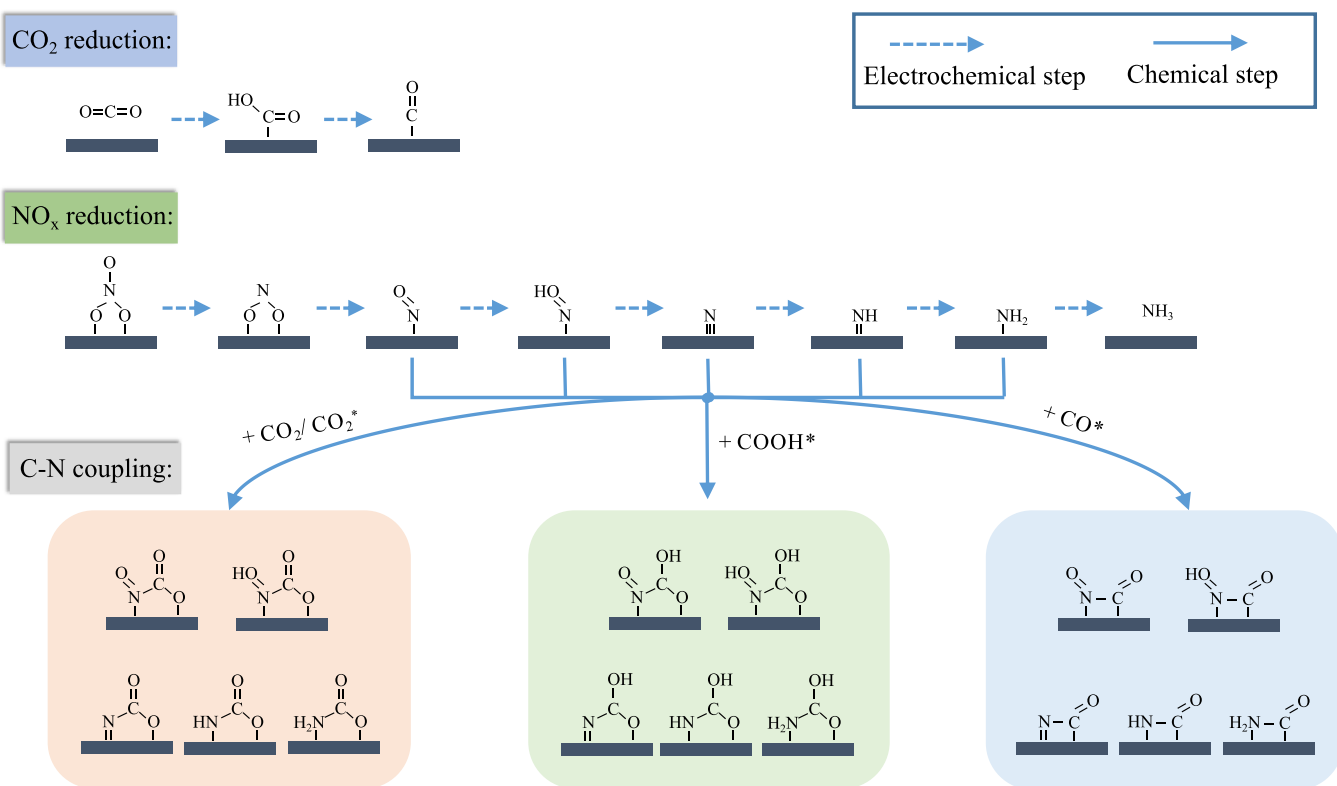


**Fig. 1.** The scheme of investigated reactions about  $\text{CO}_2$  and  $\text{NO}_x$  reduction alone and the various situations of the first C-N coupling steps in  $\text{CO}_2$  and  $\text{NO}_x$  co-reduction process.

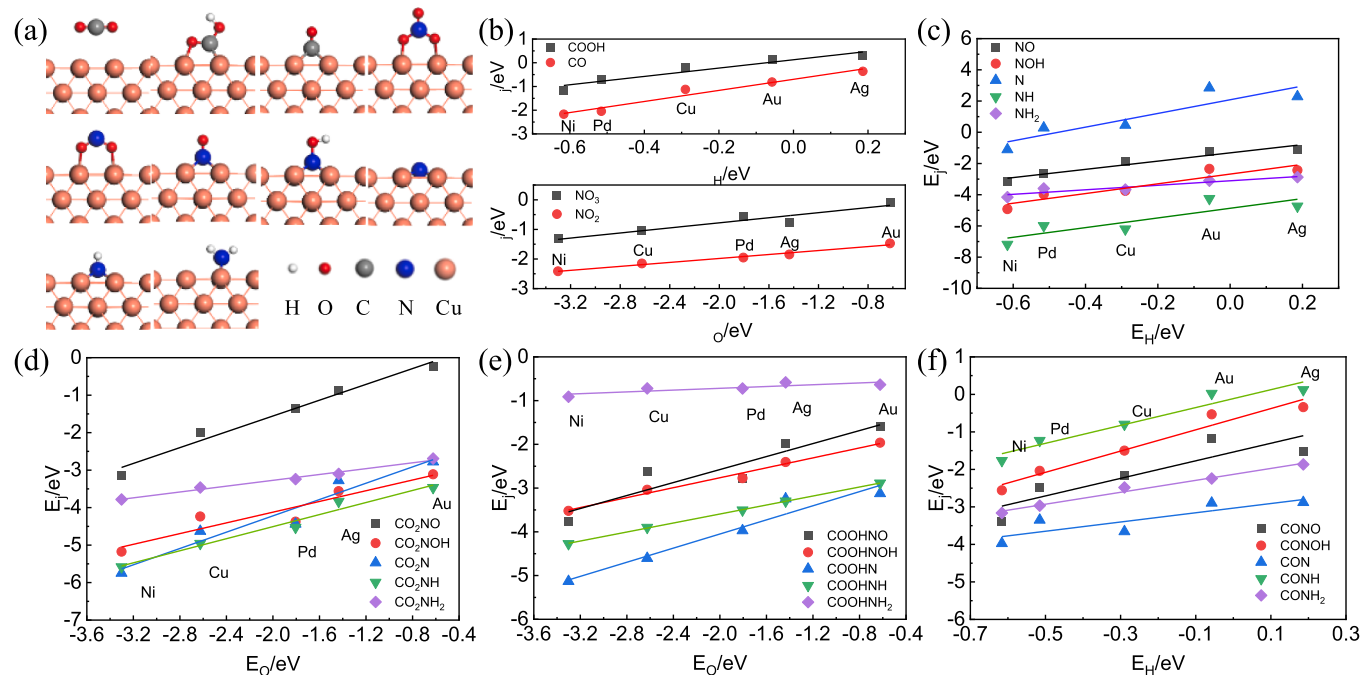


**Fig. 2.** (a) The adsorption structures of  $\text{CO}_2$ ,  $\text{COOH}^*$ ,  $\text{CO}^*$ ,  $\text{NO}_3^*$ ,  $\text{NO}_2^*$ ,  $\text{NO}^*$ ,  $\text{NOH}^*$ ,  $\text{N}^*$ ,  $\text{NH}^*$ , and  $\text{NH}_2^*$  on Cu(100) surface; the linear relationships between the adsorption energies of (b)  $\text{COOH}^*/\text{CO}^*$  and  $\text{H}^*$ ,  $\text{NO}_3^*/\text{NO}_2^*$  and  $\text{O}^*$ ; (c)  $\text{NO}^*/\text{NOH}^*$ ,  $\text{N}^*/\text{NH}^*$ ,  $\text{NH}_2^*$ , and  $\text{H}^*$ ; (d)  $\text{CO}_2\text{NO}^*/\text{CO}_2\text{NOH}^*$ ,  $\text{CO}_2\text{N}^*/\text{CO}_2\text{NH}^*$ , and  $\text{O}^*$ ; (e)  $\text{COOHNO}^*/\text{COOHN}^*$ ,  $\text{COOHN}^*/\text{COOHNH}_2^*$ , and  $\text{O}^*$ ; (e)  $\text{CONO}^*/\text{CONOH}^*$ ,  $\text{CON}^*/\text{CONH}^*$ ,  $\text{CONH}_2^*$ , and  $\text{H}^*$  on Au(100), Ag(100), Pd(100), Cu(100), Ni(100) surfaces.

oxygen can not describe the adsorption energies of  $\text{CO}_2$ . In contrast,  $\text{NO}_3^-$  and  $\text{NO}_2^-$  connect all the studied metal surfaces through oxygen atoms, and their adsorption energies are successfully described by the

$\Delta E_O$  (Fig. 2b).

The reaction sequence  $\text{NO}_3^* \rightarrow \text{NO}_2^* \rightarrow \text{NO}^* \rightarrow \text{NOH}^* \rightarrow \text{N}^* \rightarrow \text{NH}^* \rightarrow \text{NH}_2^* \rightarrow \text{NH}_3$  has been identified as the most likely reaction sequence to

form  $\text{NH}_3$  in previous studies [36,40,55]. Different from the adsorption of  $\text{NO}_3^-$  and  $\text{NO}_2^-$ , their reduction intermediates are bonded with the metal atoms by nitrogen atoms (Fig. 2a and Fig. S2). In addition, from the point view of chemical composition of urea ( $\text{CO}(\text{NH}_2)_2$ ), only  $\text{CO}_2$ ,  $\text{COOH}^*$ , and  $\text{CO}^*$  could participate in the formation of urea. The over-reduction of  $\text{CO}_2$  to form  $\text{CHO}^*$ ,  $\text{CH}^*$ ,  $\text{CH}_2^*$  etc. would lead to the side reactions, which are adverse to form urea. Thus, only the intermediates  $\text{COOH}^*$  and  $\text{CO}^*$  [56] which are bonded with the metal atoms by carbon atom are considered to bind with  $\text{N}_1$  species. Generally, the elements (N/C or O) of adsorbed species bonded with metal surface

do not change with the type of studied metals. Fig. 2b and c show that the dominant intermediate species of  $\text{NO}_x\text{RR}$  ( $\text{NO}^*$ ,  $\text{NOH}^*$ ,  $\text{N}^*$ ,  $\text{NH}^*$ , and  $\text{NH}_2^*$ ) and  $\text{CO}_2\text{RR}$  ( $\text{COOH}^*$  and  $\text{CO}^*$ ) could also be scaled with descriptor  $\Delta E_H$ . All of the adsorbate linear scaling relations have positive slopes, representing that the stronger adsorption strength of adsorbed species involved in  $\text{CO}_x$  and  $\text{NO}_x$  hydrogenation reduction reaction correlates to the stronger adsorption strength of H or O atoms (i.e., more negative  $\Delta E_H$  or  $\Delta E_O$ ).

Especially, in the electrochemical urea formation process, the potential of C-N coupling process would not obviously change with the

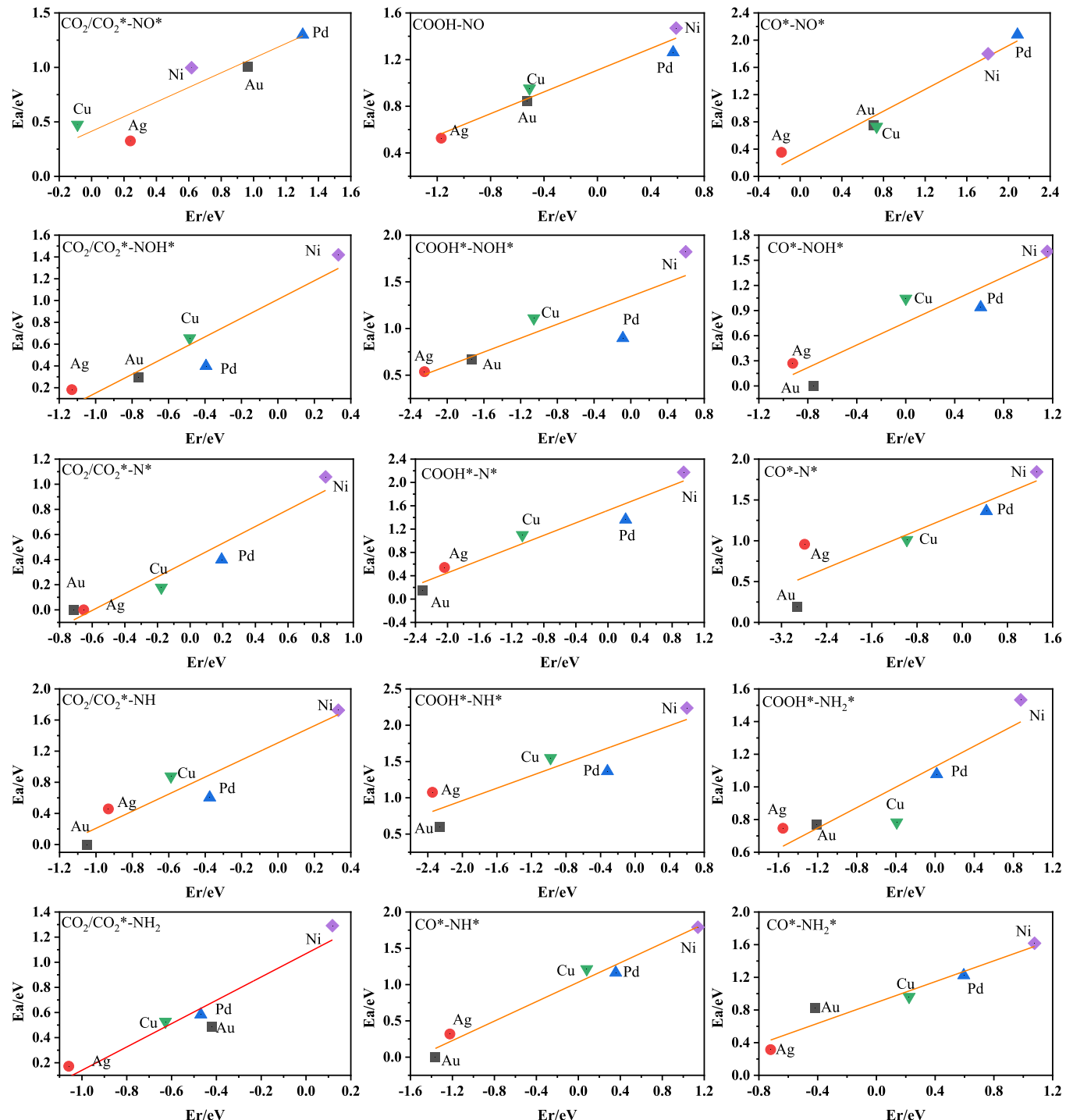


**Fig. 3.** Calculated Brønsted-Evans-Polanyi (BEP) relationships for C-N coupling by  $\text{CO}_2/\text{CO}_2^*\text{-NO}^*$ ,  $\text{CO}_2/\text{CO}_2^*\text{-NOH}^*$ ,  $\text{CO}_2\text{-N}^*$ ,  $\text{CO}_2\text{-NH}^*$ ,  $\text{CO}_2\text{-NH}_2^*$ ,  $\text{COOH}^*\text{-NO}^*$ ,  $\text{COOH}^*\text{-NOH}^*$ ,  $\text{COOH}^*\text{-N}^*$ ,  $\text{COOH}^*\text{-NH}^*$ ,  $\text{COOH}^*\text{-NH}_2^*$ ,  $\text{CO}^*\text{-NO}^*$ ,  $\text{CO}^*\text{-NOH}^*$ ,  $\text{CO}^*\text{-N}^*$ ,  $\text{CO}^*\text{-NH}^*$  and  $\text{CO}^*\text{-NH}_2^*$  at 0 V vs. RHE.

applied voltage based on the computational hydrogen electrode (CHE) model, thus C-N coupling could be the important rate-limiting steps in the electrocatalytic process. To generate the urea, the C-N bond formation reactions between three C<sub>1</sub> (CO<sub>2</sub>, COOH\*, and CO\*) species and five N<sub>1</sub> (NO\*, NOH\*, N\*, NH\*, and NH<sub>2</sub>\*) species are studied, considering the dominant CO<sub>2</sub> and NO<sub>x</sub> individual reduction pathways. Thus, the adsorptions of a total of 15 C-N coupling intermediates are carefully investigated (The adsorption configurations are shown in Fig. S3). Interestingly, the adsorption energies of C-N coupled intermediates are linearly described by  $\Delta E_H$  or  $\Delta E_O$  (Fig. 2d-f). The intermediates formed from CO<sub>2</sub>/COOH\* and N<sub>1</sub> species (NO\*, NOH\*, N\*, NH\*, and NH<sub>2</sub>\*) chemically interact with metal surfaces via N and O atom (Fig. S3), and there are not completely discrete relationships between  $\Delta E_O$  and the adsorption energies of N<sub>1</sub> species (NO\*, NOH\*, N\*, NH\*, and NH<sub>2</sub>\*) as shown in Fig. S4, so it is not surprising to see that the adsorption energies of these intermediates are linearly related by  $\Delta E_O$ . Besides, the adsorption energies of intermediates coupled by CO\* and N<sub>1</sub> species (NO\*, NOH\*, N\*, NH\*, and NH<sub>2</sub>\*) are linearly described by  $\Delta E_H$  due to the dominant interaction between molecules and metal surfaces via C and N atom. The positive slopes indicate that the order of adsorption strength of C-N intermediate species on different metal surfaces is consistent with that of H or O atoms. Therefore, the reaction energies (E<sub>r</sub>) for the C-N coupling steps could be well scaled by  $\Delta E_H$  or  $\Delta E_O$  or combinations of  $\Delta E_H$  and  $\Delta E_O$ . The corresponding functions are listed in the Supporting Information (Table S1). It could be concluded from the obtained functions that the catalysts with lower  $\Delta E_O$  (stronger adsorption of O atom) and higher  $\Delta E_H$  (weaker adsorption of H atom) would lead to lower reaction energies for all studied C-N coupling steps. Similarly, the reaction energies of hydrogenation reaction of NO<sub>x</sub> can also be described by  $\Delta E_H$  or  $\Delta E_O$  or combinations of  $\Delta E_H$  and  $\Delta E_O$  (Table S2), and the results in accord with the previously reported [40] are obtained (to form N\*, it is more beneficial for the catalysts with stronger adsorption of H and O atom, while to generate NH<sub>2</sub>\* from N\*, the catalysts with stronger adsorption of O atom and weaker adsorption of H atom is more feasible).

Besides, the energy barrier is an important determinant of the difficulty of the reaction. Brønsted-Evans-Polanyi (BEP) relation is the linear relationship between the reaction energy (E<sub>r</sub>) and energy barrier (E<sub>a</sub>) of the elementary step on different catalysts. In previous research, BEP relations have been verified in all elementary steps of CO<sub>x</sub>RR and NO<sub>x</sub>RR [40,55]. To describe the catalysis performance of metals on CO<sub>2</sub> and NO<sub>x</sub> co-reduction, we present evidence for the existence of BEP relations between  $\Delta E_r$  and  $\Delta E_a$  for the C-N coupling steps as shown in Fig. 3 (The structures of transition states are displayed in Fig. S5). The results also suggest that the energy barriers of the most of C-N coupling steps on the Ni surface are the highest, whereas Ag and Au have the lowest energy

barrier.

### 3.2. Mechanism of CO<sub>2</sub> and NO<sub>x</sub> co-reduction reaction

For the electrocatalytic urea formation by CO<sub>2</sub> and NO<sub>x</sub> co-reduction involving multiple electrochemical and non-electrochemical steps, it is essential to clarify the reaction mechanism to give insights into the catalyst design. However, the intermediates from which the C-N bond is derived from in urea synthesis are still controversial [34].

Here we calculated the energy barriers including electrochemical and non-electrochemical steps until the completion of C-N coupling, and the energy barriers of electrochemical steps at -1.0 V vs. RHE are obtained on the basis of the CHE model and Butler-Volmer formalism [53] (Fig. 4 and Figs. S6-S10). Fig. 4d shows that CO<sub>2</sub> is generally more feasible to bond with N<sub>1</sub> species than COOH\* and CO\* and the C-N coupling step by CO<sub>2</sub>+N\* has the lowest energy barrier than other C-N coupling steps on the Cu surface, which is corresponding to the previous research [36]. On other surfaces, there are similar results that CO<sub>2</sub>/CO<sub>2</sub>\* to bond with intermediates N\* is advantageous from the perspective of energy barrier.

To further identify the reaction mechanism of electrocatalytic urea production, the micro-kinetic analysis is performed to comprehensively consider the thermodynamic and kinetic properties of various C-N bonding pathways. Fig. 5 shows the results of the coverage of C-N bonding intermediates on investigated metal surfaces at -1.0 V vs. RHE (The situations at -1.0 V vs. RHE will be introduced here since the applied voltage of -1.0 V vs. RHE is close to -1.5 V vs. SHE in the reported experiments [9]). It could be concluded from Fig. 5 that CO<sub>2</sub>NO\*, CO<sub>2</sub>NOH\*, or CO<sub>2</sub>N\* occupies most active sites at equilibrium state on the Au (100), Ag (100), Pd (100), and Cu (100) surfaces, which means that the C-N bond is dominantly formed from CO<sub>2</sub> and N<sub>1</sub> species (NO\*, NOH\* or N\*) on these surfaces. In contrast, on Ni(100) surface, the intermediate CON\* occupies most active sites than other C-N coupling intermediates, which results from that the chemically adsorbed CO<sub>2</sub> is more feasible to be reduced than bonded with adsorbed N<sub>1</sub> species. In addition, the order of largest coverage values at equilibrium state of C-N bonding intermediates on these metal surfaces is Cu (0.86 ML) > Ag (0.25 ML) > Au (1.67 × 10<sup>-6</sup> ML) > Pd (4.19 × 10<sup>-11</sup> ML) > Ni (1.29 × 10<sup>-24</sup> ML), which suggest that the order of catalysis performance of metal surfaces for electrochemical urea synthesis, in agreement with the previous experimental reports (Table S3) [9]. The clarification about the C-N bonding reaction mechanism is helpful to quickly determine the efficient catalysts. It could be preliminary concluded that the metal surfaces leading to chemically adsorbed CO<sub>2</sub> are unfavorable to electrochemical urea synthesis.

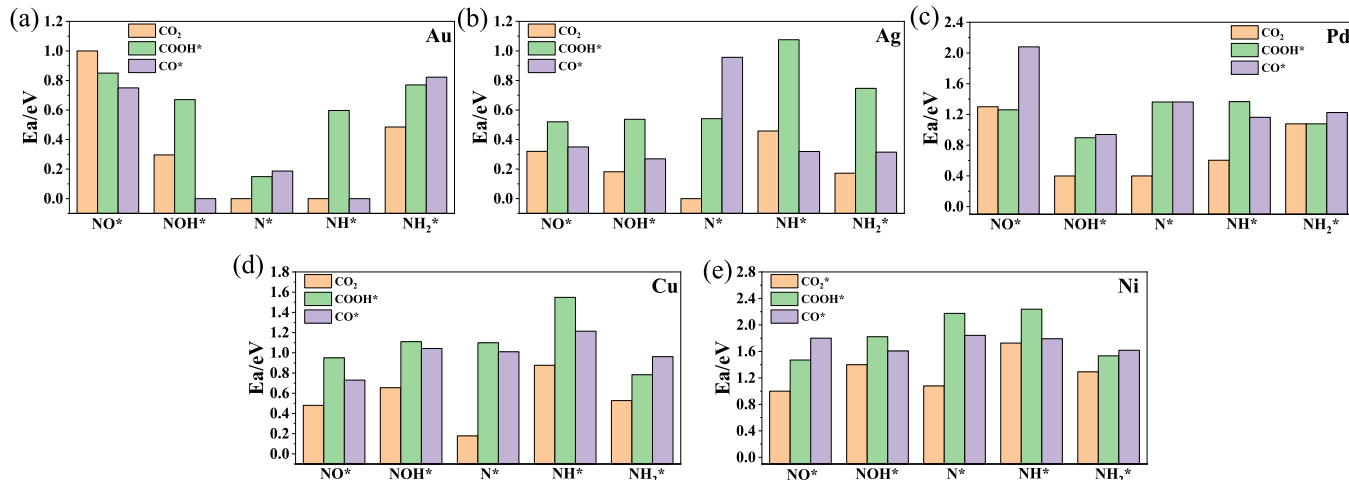


**Fig. 4.** The energy barriers of C-N bonding reactions on (a) Au (100); (b) Ag (100); (c) Pd (100); (d) Cu (100); (e) Ni (100) surfaces.

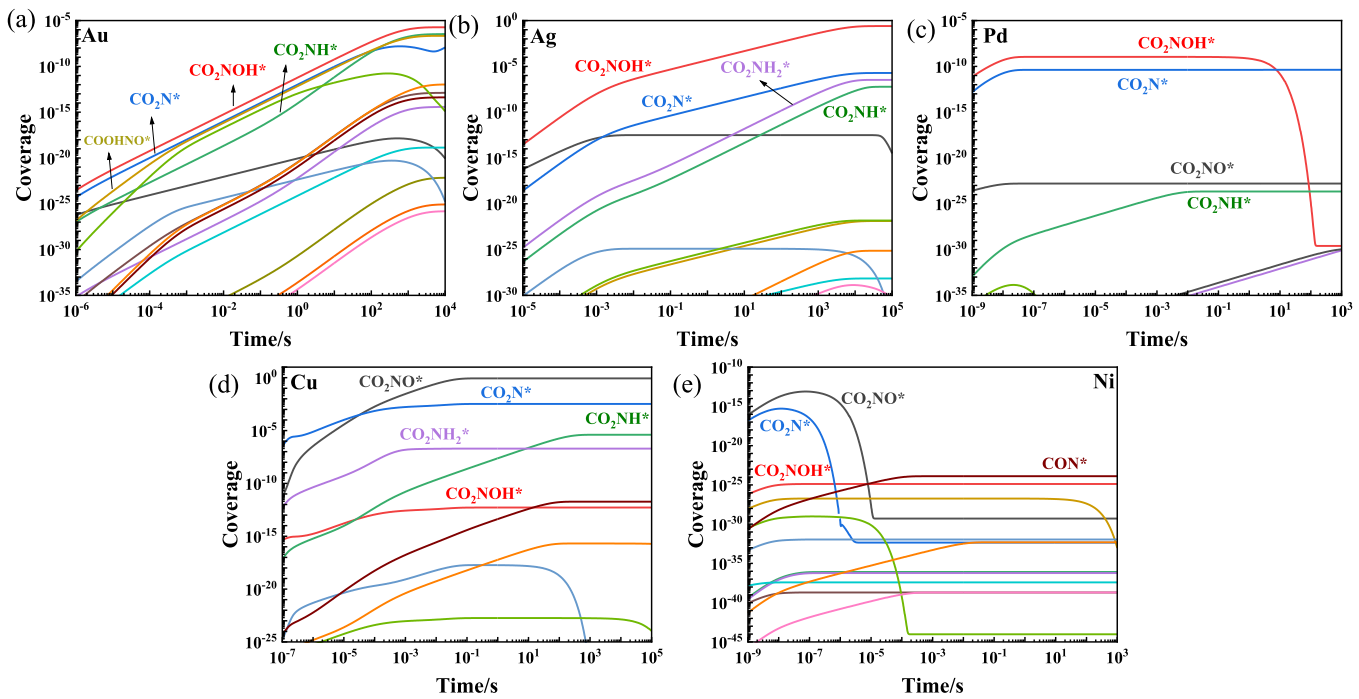


**Fig. 5.** The coverage of C-N bonding intermediates on (a) Au (100); (b) Ag (100); (c) Pd (100); (d) Cu (100); (e) Ni (100) surfaces at  $-1.0$  V vs. RHE.

### 3.3. Guidance for catalyst screening

Based on the proposed descriptors and reaction mechanism, it is possible to formulate the guidance to screen and design catalysts for electrochemical urea synthesis from multiple perspectives.  $\text{CO}_2$  is the reactant and the important intermediate involved in the C-N coupling step. The chemical adsorption of  $\text{CO}_2$  on metal surfaces (Ni as an example) is prejudicial due to the smaller  $\text{CO}_2/\text{CO}_2^*$  concentration, lowered energy barrier of reduction but increased energy barrier of C-N bonding compared to physical adsorption (such as Au, Ag, Pd, and Cu). Indeed, whatever nitrate or nitrite as the reactant, the formation of urea with Ni at the gas-diffusion electrode was not found in the reported experimental results. Thus, the formed chemical adsorption of  $\text{CO}_2$  can be proposed as an indicator of the metal surfaces with poor catalysis performance during the screening. To further validate this indicator, the adsorption of  $\text{CO}_2$  on Cr, Mo, Co, Rh, Ir, Pt, Zn, Cd, and In are theoretically investigated as well, with the adsorption structures and adsorption energies displayed in Fig. S11 and Table S3. Stable chemical adsorptions of  $\text{CO}_2$  were shown on Cr, Mo, Co, Rh and Ir. Interestingly, it was experimentally reported that these metals as electrocatalysts can not produce urea even with nitrite as the reactant [8,9]. In contrast,  $\text{CO}_2$  was found to be physically adsorbed on the Zn, Cd, and In, which exhibit electrocatalytic performance for urea production in experiments [8,9]. Specially,  $\text{CO}_2$  is also physically adsorbed on Pt while Pt could not catalyze the electro-production of urea, which will be explained by the proposed descriptors later.

The  $\text{CO}_2$  adsorption can only help researchers quickly exclude the metal catalysts with extremely poor catalysis performance. To conveniently and feasibly identify the catalysts with excellent catalysis performance, a screening method based on both  $\Delta E_H$  and  $\Delta E_O$  descriptors is proposed on the basis of the linear relationship with  $E_a$  and the elucidated reaction mechanism (all the  $\Delta E_H$  and  $\Delta E_O$  of investigated metals are listed in Table S3). The reaction process to complete C-N bond formation from  $\text{CO}_2$  and  $\text{NO}_x$  could be divided into three parts. The first part is the adsorption of reactants. For the reactant  $\text{CO}_2$ , it has been determined that it should be physically adsorbed on the metal surface, whereas the reactant  $\text{NO}_x$  should be chemically adsorbed to facilitate further reduction and the adsorption energy of  $\text{NO}_x$  is linearly related to

the  $\Delta E_O$ . Hence, to increase the reactant concentration on the catalysis surface, the metal surface should have strong oxygen adsorption (lower  $\Delta E_O$ ). The second part to be considered is the reduction of  $\text{NO}_x^*$  to  $\text{NO}^*$ ,  $\text{NOH}^*$  and  $\text{N}^*$ , since  $\text{NO}^*$ ,  $\text{NOH}^*$  and  $\text{N}^*$  are generally the intermediates to bond with  $\text{CO}_2$  as shown by the reaction mechanism. According to the reported BEP relationships in the  $\text{NO}_x$  reduction process which are also verified in this work (Fig. S12), both the reaction energies and energy barriers are described by liner combinations of  $\Delta E_H$  and  $\Delta E_O$ , and the functions (Table S2) indicate that the lower  $\Delta E_H$  and  $\Delta E_O$  correspond to lower reaction energies and energy barriers for every elementary step from  $\text{NO}_x^*$  to  $\text{N}^*$ . Thirdly, the catalysts must have the low energy barrier of the C-N coupling step since it is the non-electrochemical step. Based on the obtained functions in Table S1, the higher  $\Delta E_H$  and lower  $\Delta E_O$  represent a lower energy barrier. Overall, the catalysts with moderate hydrogen and strong oxygen adsorption strength are predicted with outstanding catalysis performance. In this regard, the poor catalysis performance of Pt is considered to be due to the over-strong adsorption of the H atom. And the metal surfaces (Cr, Mo, Co, Rh, Ir and Ni) with chemical adsorption of  $\text{CO}_2$  corresponding to both strong H and O atom adsorption strength, the metal surfaces (such as Zn) with strong O atom adsorption without strong H atom adsorption can't lead to the chemical adsorption of  $\text{CO}_2$  (Note: There is no extremely strong O adsorption to only bond with O atom of  $\text{CO}_2$  for the transition metals with moderate H adsorption based on the d band center theory [57]), thus, it explains the reason that the  $\text{CO}_2$  adsorption can help researchers directly exclude the metal catalysts with poor catalysis performance. To validate the proposed guidance, the volcano plots of experimentally reported Faradic efficiency of electrochemical urea formation from  $\text{CO}_2$  and nitrate or nitrite (at  $-1.5$  V vs SHE [9]) as a function of theoretical  $\Delta E_H$  and  $\Delta E_O$  from DFT calculations on various metals are plotted in Fig. 6. Obviously, the proposed screening guidance is indeed in line with the experimental results.

### 4. Conclusions

In summary, this work investigated the adsorption energies, reaction energies, and energy barriers involved in C-N coupling process on Au, Ag, Pd, Cu, and Ni surfaces on the basis of DFT calculations. The

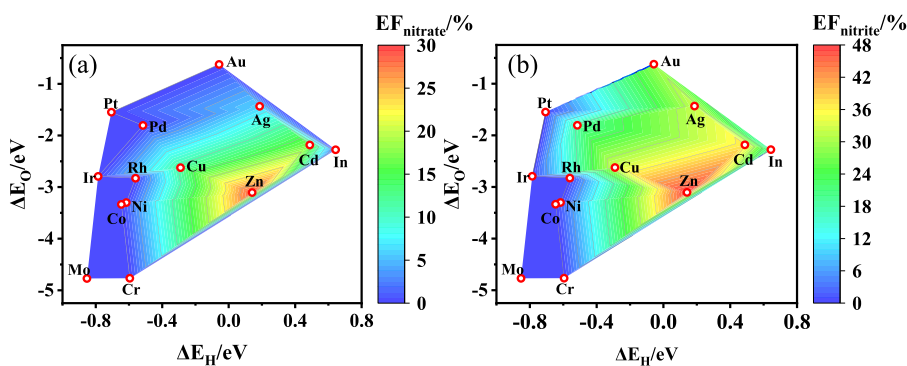


**Fig. 6.** The volcano plots of experimentally reported Faradic efficiency of electrochemical urea formation (at  $-1.5$  V vs SHE) from  $\text{CO}_2$  and (a) nitrate or (b) nitrite as a function of theoretical  $\Delta E_{\text{H}}$  and  $\Delta E_{\text{O}}$  from DFT calculations on various metals.

adsorption energies of C-N intermediates could be linearly related by the adsorption energies of H or O atom ( $\Delta E_{\text{H}}$  or  $\Delta E_{\text{O}}$ ). Considering that there is also linear relationship between the adsorption energies of reactants about C-N bonding steps and  $\Delta E_{\text{H}}$  or  $\Delta E_{\text{O}}$ , the reaction energies ( $E_r$ ) are well described by linear combinations of  $\Delta E_{\text{H}}$  and  $\Delta E_{\text{O}}$ . Moreover, the Brønsted-Evans-Polanyi (BEP) relation was verified for C-N coupling reactions, which represents the energy barriers ( $E_a$ ) have the same trend as  $E_r$  with the change of  $\Delta E_{\text{H}}$  and  $\Delta E_{\text{O}}$ . The micro-kinetic analysis suggests that the C-N formation mechanism is more feasible by  $\text{CO}_2$  and N1 species ( $\text{NO}^*$ ,  $\text{NOH}^*$  or  $\text{N}^*$ ). It is found that the strong adsorption of  $\text{CO}_2$  is adverse to the C-N bonding, and the chemical adsorption state of  $\text{CO}_2$  on the surface has been proposed as a indicator to directly identify the catalysts with very poor performance. Based on the calculations, Cu and Ag are more efficient to catalyze electrochemical generation of urea than Au, Pd, and Ni, which is in line with the experimental results [9]. Furthermore, based on the proposed descriptors and reaction mechanism, the catalysts with the moderate hydrogen and strong oxygen adsorption strength are predicted with the outstanding catalysis performance by considering all the steps including the adsorption of nitrate/nitrite, reduction of nitrate/nitrite, and C-N coupling. This screening guidance could be verified by the experimental results.

Overall, this work simplifies the complicated process by descriptors, reveals the C-N coupling mechanism, and proposes the catalysts screen guidance, which might facilitate the development of high-performance catalysts for electrocatalytic urea synthesis.

#### CRediT authorship contribution statement

**Meng Zheng:** Conceptualization, Methodology, Writing – original draft preparation. **Haiqing Ma:** Conceptualization, Supervision. **Zhiming Li:** Methodology, Writing – review & editing. **Hongan Yu:** Formal analysis, Data curation. **Long Nie:** Formal analysis, Data curation. **Chenliang Ye:** Writing – review & editing. **Xiaoyu Chen:** Writing – review & editing. **Jin Wang:** Conceptualization, Supervision, Funding acquisition.

#### Declaration of Competing Interest

The authors declare no competing financial interest.

#### Data availability

Data will be made available on request.

#### Acknowledgments

This work was financially supported by Natural Science Foundation of China (22022508) and National Key R&D Program of China (2021YFA1600800).

#### Appendix A. Supporting information

Supplementary data associated with this article can be found in the online version at doi:10.1016/j.apcatb.2023.123366.

#### References

- [1] J.W. Erisman, M.A. Sutton, J. Galloway, Z. Klimont, W. Winiarwter, How a century of ammonia synthesis changed the world, *Nat. Geosci.* 1 (2008) 636–639.
- [2] Y. Zhong, H. Xiaong, J. Low, R. Long, Y. Xiong, Recent progress in electrochemical C–N coupling reactions, *eScience* (2023), 100086.
- [3] Z.Y. Wu, M. Karamad, X. Yong, Q. Haung, Q.A. Cullen, P. Zhu, C. Xia, Q. Xiao, M. Shakouri, F.Y. Chen, H.Y. Kim, Y. Xia, K. Heck, Y. Hu, M.S. Wong, Q. Li, I. Gates, S. Siahrostami, H. Wang, Electrochemical ammonia synthesis via nitrate reduction on Fe single atom catalyst, *Nat. Commun.* 12 (2021) 2870.
- [4] Y. Zhai, P. Han, Q. Yun, Y. Ge, X. Zhang, Y. Chen, H. Zhang, Phase engineering of metal nanocatalysts for electrochemical  $\text{CO}_2$  reduction, *eScience* (2022) 467–485.
- [5] X. Fan, L. Xie, J. Liang, Y. Ren, L. Zhang, L. Yue, T. Li, Y. Luo, N. Li, B. Tang, Y. Liu, S. Gao, A.A. Alshehri, Q. Liu, Q. Kong, X. Sun, In situ grown  $\text{Fe}_3\text{O}_4$  particle on stainless steel: a highly efficient electrocatalyst for nitrate reduction to ammonia, *Nano Res.* 15 (2022) 3050–3055.
- [6] Z. Zhang, Y. Liu, X. Su, Z. Zhao, Z. Mo, C. Wang, Y. Zhao, Y. Chen, S. Gao, Electro-triggered joule heating method to synthesize single-phase CuNi nano-alloy catalyst for efficient electrocatalytic nitrate reduction toward ammonia, *Nano Res.* (2023), <https://doi.org/10.1007/s12274-023-5402-y>.
- [7] M. Shibata, K. Yoshida, N. Furuya, Electrochemical synthesis of urea at gas-diffusion electrodes Part II. Simultaneous reduction of carbon dioxide and nitrite ions at Cu, Ag and Au catalysts, *J. Electroanal. Chem.* 442 (1998) 67–72.
- [8] M. Shibata, K. Yoshida, N. Furuya, Electrochemical synthesis of urea at gas-diffusion electrodes III. Simultaneous reduction of carbon dioxide and nitrite ions with various metal catalysts, *J. Electrochem. Soc.* 145 (1998) 595–600.
- [9] M. Shibata, K. Yoshida, N. Furuya, Electrochemical synthesis of urea at gas-diffusion electrodes IV. Simultaneous reduction of carbon dioxide and nitrate ions with various metal catalysts, *J. Electrochem. Soc.* 145 (1998) 2348–2353.
- [10] M. Shibata, N. Furuya, Electrochemical synthesis of urea at gas-diffusion electrodes Part VI. Simultaneous reduction of carbon dioxide and nitrite ions with various metallophthalocyanine catalysts, *J. Electroanal. Chem.* 507 (2001) 177–184.
- [11] M. Shibata, N. Furuya, Simultaneous reduction of carbon dioxide and nitrate ions at gasdiffusion electrodes with various metallophthalocyanine catalysts, *Electrochim. Acta* 48 (2003) 3953–3958.
- [12] P.M. Krzywda, A.P. Rodríguez, N.E. Benes, B.T. Mei, G. Mul, Carbon-nitrogen bond formation on Cu electrodes during  $\text{CO}_2$  reduction in  $\text{NO}_3^-$  solution, *Appl. Catal. B: Environ.* 316 (2022), 121512.
- [13] X. Liu, P.V. Kumar, Q. Chen, L. Zhao, F. Ye, X. Ma, D. Liu, X. Chen, L. Dai, C. Hu, Carbon nanotubes with fluorine-rich surface as metal-free electrocatalyst for effective synthesis of urea from nitrate and  $\text{CO}_2$ , *Appl. Catal. B: Environ.* 316 (2022), 121618.
- [14] Z. Shi, J. Chen, K. Li, Y. Liu, Y. Tang, L. Zhang, Flue gas to urea: a path of flue gas resourceful utilization through electrocatalysis, *Chem. Eng. J.* 461 (2023), 141933.
- [15] H. Wang, Y. Jiang, S. Li, F. Gou, X. Liu, Y. Jiang, W. Luo, W. Shen, R. He, M. Li, Realizing efficient C–N coupling via electrochemical co-reduction of  $\text{CO}_2$  and  $\text{NO}_3^-$  on AuPd nanoalloy to form urea: Key C–N coupling intermediates, *Appl. Catal. B: Environ.* 318 (2022), 121819.
- [16] J. Qin, N. Liu, L. Chen, K. Wu, Q. Zhao, B. Liu, Z. Ye, Selective electrochemical urea synthesis from nitrate and  $\text{CO}_2$  using in situ ru anchoring onto a three-dimensional copper electrode, *ACS Sustain. Chem. Eng.* 10 (2022) 15869–15875.
- [17] J. Leverett, T. Tran-Phu, J.A. Yuwono, P. Kumar, C. Kim, Q. Zhai, C. Han, J. Qu, J. Cairney, A.N. Simonov, R.K. Hocking, L. Dai, R. Daiyan, R. Amal, Tuning the coordination structure of Cu–N–C single atom catalysts for simultaneous electrochemical reduction of  $\text{CO}_2$  and  $\text{NO}_3^-$  to urea, *Adv. Energy Mater.* 12 (2022) 2201500.

[18] N. Meng, Y. Huang, Y. Liu, Y. Yu, B. Zhang, Electrosynthesis of urea from nitrite and CO<sub>2</sub> over oxygen vacancy-rich ZnO porous nanosheets, *Cell Rep. Phys. Sci.* 2 (2021), 100378.

[19] D. Saravanakumar, J. Song, S. Lee, N.H. Hur, W. Shin, Electrocatalytic conversion of carbon dioxide and nitrate ions to urea by a titania-nafion composite electrode, *ChemSusChem* 10 (2017) 3999–4003.

[20] C. Lv, L. Zhong, H. Liu, Z. Fang, C. Yan, M. Chen, Y. Kong, C. Lee, D. Liu, S. Li, J. Liu, L. Song, G. Chen, Q. Yan, G. Yu, Selective electrocatalytic synthesis of urea with nitrate and carbon dioxide, *Nat. Sustain.* 4 (2021) 868–876.

[21] N. Cao, Y. Quan, A. Guan, C. Yang, Y. Ji, L. Zhang, G. Zheng, Oxygen vacancies enhanced cooperative electrocatalytic reduction of carbon dioxide and nitrite ions to urea, *J. Colloid Interf. Sci.* 577 (2020) 109–114.

[22] Y. Feng, H. Yang, Y. Zhang, X. Huang, L. Li, T. Cheng, Q. Shao, Te-Doped Pd nanocrystal for electrochemical urea production by efficiently coupling carbon dioxide reduction with nitrite reduction, *Nano Lett.* 20 (2020) 8282–8289.

[23] D. Zhang, Y. Xue, X. Zheng, C. Zhang, Y. Li, Multi-heterointerfaces for selective and efficient urea production, *Natl. Sci. Rev.* 10 (2023) nwac209.

[24] X. Wei, Y. Liu, X. Zhu, S. Bo, L. Xiao, C. Chen, T.T.T. Nga, Y. He, M. Qiu, C. Xie, D. Wang, Q. Liu, F. Dong, C.L. Dong, X.Z. Fu, S. Wang, Dynamic reconstitution between copper single atoms and clusters for electrocatalytic urea synthesis, *Adv. Mater.* (2023) 2300020.

[25] M. Qiu, X. Zhu, S. Bo, K. Cheng, N. He, K. Gu, D. Song, C. Chen, X. Wei, D. Wang, Y. Liu, S. Li, X. Tu, Y. Li, Q. Liu, C. Li, S. Wang, Boosting electrocatalytic urea production via promoting asymmetric C-N coupling, *CCS Chem.* (2023), <https://doi.org/10.31635/ccschem.023.202202408>.

[26] X. Zhang, X. Zhu, S. Bo, C. Chen, M. Qiu, X. Wei, N. He, C. Xie, W. Chen, J. Zheng, P. Chen, S.P. Jiang, Y. Li, Q. Liu, S. Wang, Identifying and tailoring C-N coupling site for efficient urea synthesis over diatomic Fe-Ni catalyst, *Nat. Commun.* 13 (2022) 5337.

[27] X. Wei, X. Wen, Y. Liu, C. Chen, C. Xie, D. Wang, M. Qiu, N. He, P. Zhou, W. Chen, J. Cheng, H. Lin, J. Jia, X.Z. Fu, S. Wang, Oxygen vacancy-mediated Selective C-N coupling toward electrocatalytic urea synthesis, *J. Am. Chem. Soc.* 144 (2022) 11530–11535.

[28] C. Lv, C. Lee, L. Zhong, H. Liu, J. Liu, L. Yang, C. Yan, W. Yu, H.H. Hng, Z. Qi, L. Song, S. Li, K.P. Loh, Q. Yan, G. Yu, A defect engineered electrocatalyst that promotes high-efficiency urea synthesis under ambient conditions, *ACS Nano* 16 (2022) 8213–8222.

[29] N. Meng, X. Ma, C. Wang, Y. Wang, R. Yang, J. Shao, Y. Huang, Y. Xu, B. Zhang, Y. Yu, Oxide-derived core-shell Cu@Zn nanowires for urea electrosynthesis from carbon dioxide and nitrate in water, *ACS Nano* 16 (2022) 9095–9104.

[30] X. Liu, P.V. Kumar, Q. Chen, L. Zhao, F. Ye, X. Ma, D. Liu, X. Chen, L. Dai, C. Hu, Carbon nanotubes with fluorine-rich surface as metal-free electrocatalyst for effective synthesis of urea from nitrate and CO<sub>2</sub>, *Appl. Catal. B: Environ.* 316 (2022), 121618.

[31] H. Wang, Y. Jiang, S. Li, F. Gou, X. Liu, Y. Jiang, W. Luo, W. Shen, R. He, M. Li, Realizing efficient C-N coupling via electrochemical co-reduction of CO<sub>2</sub> and NO<sub>3</sub><sup>-</sup> on AuPd nanoalloy to form urea: key C-N coupling intermediates, *Appl. Catal. B: Environ.* 318 (2022), 121819.

[32] C. Lv, C. Lee, L. Zhong, H. Liu, J. Liu, L. Yang, C. Yan, W. Yu, H.H. Hng, Z. Qi, L. Song, S. Li, K.P. Loh, Q. Yan, G. Yu, A defect engineered electrocatalyst that promotes high-efficiency urea synthesis under ambient conditions, *ACS Nano* 16 (2022) 8213–8222.

[33] J. Li, Y. Zhang, K. Kuruvinashetti, N. Kornienko, Construction of C-N bonds from small-molecule precursors through heterogeneous electrocatalysis, *Nat. Rev. Chem.* 6 (2022) 303–319.

[34] C. Chen, N. He, S. Wang, Electrocatalytic C-N coupling for urea synthesis, *Small Sci.* 1 (2021) 2100070.

[35] X. Liu, Y. Jiao, Y. Zheng, M. Jaroniec, S.Z. Qiao, Mechanism of C-N bonds formation in electrocatalytic urea production revealed by ab initio molecular dynamics simulation, *Nat. Commun.* 13 (2022) 5471.

[36] G.L. Yang, C.T. Hsieh, Y.S. Ho, T.C. Kuo, Y. Kwon, Q. Lu, M.J. Cheng, Gaseous CO<sub>2</sub> coupling with N-Containing intermediates for key C-N bond formation during urea production from coelectrolysis over Cu, *ACS Catal.* 12 (2022) 11494–11504.

[37] J.K. Nørskov, T. Bligaard, A. Logadottir, J.R. Kitchin, J.G. Chen, S. Pandelov, U. Stimming, Trends in the exchange current for hydrogen evolution, *J. Electrochem. Soc.* 152 (2005) J23–J26.

[38] J.K. Nørskov, J. Rossmeisl, A. Logadottir, L. Lindqvist, Origin of the overpotential for oxygen reduction at a fuel-cell cathode, *J. Phys. Chem. B* 108 (2004) 17886–17892.

[39] J. Schumann, A.J. Medford, J.S. Yoo, Z.J. Zhao, P. Bothra, A. Cao, F. Studt, F. Abild-Pedersen, J.K. Nørskov, Selectivity of synthesis gas conversion to C<sub>2+</sub> oxygenates on fcc[111] transition-metal surfaces, *ACS Catal.* 8 (2018) 3447–3453.

[40] J.X. Liu, D. Richards, N. Singh, B.R. Goldsmith, Activity and selectivity trends in electrocatalytic nitrate reduction on transition metals, *ACS Catal.* 9 (2019) 7052–7064.

[41] Y.G. Kim, A. Javier, J.H. Baricuatro, D. Torelli, K.D. Cummins, C.F. Tsang, J. C. Hemminger, M.P. Soriaga, Surface reconstruction of pure-Cu single-crystal electrodes under CO-reduction potentials in alkaline solutions: a study by serial tomography-DEMS, *J. Electroanal. Chem.* 780 (2016) 290–295.

[42] Y.G. Kim, J.H. Baricuatro, M.P. Soriaga, Surface reconstruction of polycrystalline Cu electrodes in aqueous KHCO<sub>3</sub> electrolyte at potentials in the early stages of CO<sub>2</sub> reduction, *Electrocatalysis* 9 (2018) 526–530.

[43] Y.G. Kim, J.H. Baricuatro, A. Javier, J.M. Gregoire, M.P. Soriaga, The evolution of the polycrystalline copper surface, first to Cu(111) and then to Cu(100), at a fixed CO<sub>2</sub>RR potential: a study by operando EC-STM, *Langmuir* 30 (2014) 15053–15056.

[44] H. Wan, X. Wang, L. Tan, M. Filippi, P. Strasser, J. Rossmeisl, A. Bagger, Electrochemical synthesis of urea: Co-reduction of nitric oxide and carbon monoxide, *ACS Catal.* 13 (2023) 1926–1933.

[45] S. Liu, H. Tao, L. Zeng, Q. Liu, Z. Xu, Q. Liu, J.L. Luo, Shape-dependent electrocatalytic reduction of CO<sub>2</sub> to CO on triangular silver nanoplates, *J. Am. Chem. Soc.* 139 (2017) 2160–2163.

[46] G. Kresse, J. Furthmüller, Efficiency of ab-initio total energy calculations for metals and semiconductors using a plane-wave basis set, *Comput. Mater. Sci.* 6 (1996) 15–50.

[47] G. Kresse, J. Furthmüller, Efficient iterative schemes for ab initio total-energy calculations using a plane-wave basis set, *J. Phys. Rev. B: Condens. Matter Mater. Phys.* 54 (1996) 11169–11186.

[48] G. Henkelman, H. Jonsson, Improved tangent estimate in the nudged elastic band method for finding minimum energy paths and saddle points, *J. Chem. Phys.* 111 (1999) 7010–7022.

[49] M. Zheng, L. Zhao, L. Cao, J. Gao, C. Xu, The combined DFT and microkinetics methods to investigate the favorite sulfur vacancies of Co[Ni]MoS<sub>2</sub> catalysts for maximizing HDS/HYDRO selectivity, *Appl. Catal. B: Environ.* 277 (2020), 119242.

[50] F. Calle-Vallejo, M. Huang, J.B. Henry, M.T.M. Koper, A.S. Bandarenka, Theoretical design and experimental implementation of Ag/Au electrodes for the electrochemical reduction of nitrate, *Phys. Chem. Chem. Phys.* 15 (2013) 3196–3202.

[51] D.Y. Shin, D.H. Lim, DFT investigation into efficient transition metal single-atom catalysts supported on N-doped graphene for nitrate reduction reactions, *Chem. Eng. J.* 468 (2023), 143466.

[52] M. Zheng, J. Wang, Regulating the oxygen affinity of single atom catalysts by dual-atom design for enhanced oxygen reduction reaction activity, *Chem. Res. Chin. Univ.* 38 (2022) 1275–1281.

[53] G. Rostamikia, A.J. Mendoza, M.A. Hickner, M.J. Janik, First-principles based microkinetic modeling of borohydride oxidation on a Au [1 1 1] electrode, *J. Power Sources* 196 (2011) 9228–9237.

[54] R.A. van Santen, A.J. Markvoort, I.A. Filot, M.M. Ghouri, E.J. Hensen, Mechanism and microkinetics of the Fischer-Tropsch reaction, *Phys. Chem. Chem. Phys.* 15 (2013) 17038–17063.

[55] J. Long, S. Chen, Y. Zhang, C. Guo, X. Fu, D. Deng, J. Xiao, Direct electrochemical ammonia synthesis from nitric oxide, *Angew. Chem. Int. Ed.* 59 (2020) 9711–9718.

[56] X. Liu, J. Xiao, H. Peng, X. Hong, K. Chan, J.K. Nørskov, Understanding trends in electrochemical carbon dioxide reduction rates, *Nat. Commun.* 8 (2017) 15438.

[57] A.J. Medford, P.G. Moses, K.W. Jacobsen, A.A. Peterson, A career in catalysis: jens kehlet nørskov, *ACS Catal.* 12 (2022) 9679–9689.